

CHARACTERIZATION OF SOLVENT EFFECTS ON C=O STRETCHING VIBRATIONS OF KETOPROFEN BY EMPIRICAL SOLVENT PARAMETERS****S. Sagdinc, N. Tekin****Kocaeli University, Kocaeli 41001, Turkey;**e-mail: seda.sagdinc@kocaeli.edu.tr; nalan.tekin@kocaeli.edu.tr*

The solvent effects on C=O stretching vibrational frequency, $\nu(\text{C=O})$, of ketoprofen (KETO) were studied experimentally using attenuated total reflection infrared spectroscopy (ATR-IR). The experimental $\nu(\text{C=O})$ of KETO were correlated with empirical solvent parameters, including the Kirkwood–Bauer–Magat (KBM) equation, the acceptor numbers (ANs) of the solvents, the Swain equation, linear solvation energy relationships (LSERs), and the quadratic equation (QE). The solvent-induced $\nu(\text{C=O})$ shifts of KETO displayed a better correlation with the LSER equation than with the KBM equation, ANs of the solvents, and the Swain equation. The linear effect of the solvent hydrogen-bond donor acidity (A_j) on $\nu(\text{C=O})$ of KETO was found to be highly significant, whereas the hydrogen-bond acceptor basicity (B_j) and the interaction effect of A_j and B_j were not significant. It was also observed that the quadratic effects of A_j and B_j were slightly significant. Additionally, the linear effect of LSER parameters (π^ , δ , α , and β) and the interaction effect of $\pi^*\beta$ on the $\nu(\text{C=O})$ of KETO were highly significant.*

Keyword: ketoprofen, solvent effect, Swain equation, linear solvation energy relationship, quadratic equation.

ХАРАКТЕРИСТИКА ВЛИЯНИЯ РАСТВОРИТЕЛЯ НА ВАЛЕНТНЫЕ КОЛЕБАНИЯ C=O КЕТОПРОФЕНА С ПОМОЩЬЮ ЭМПИРИЧЕСКИХ ПАРАМЕТРОВ РАСТВОРИТЕЛЯ**S. Sagdinc, N. Tekin***

УДК 539.194

*Университет Коджаэли, Коджаэли, 41380, Турция;**e-mail: seda.sagdinc@kocaeli.edu.tr, nalan.tekin@kocaeli.edu.tr**(Поступила 6 апреля 2020)*

С использованием инфракрасной спектроскопии ослабленного полного отражения (ATR-IR) экспериментально изучено влияние растворителя на частоту колебаний растяжения связей C=O ($\nu(\text{C=O})$) кетопрофена (KETO). Экспериментальное значение $\nu(\text{C=O})$ KETO скоррелировано с эмпирическими параметрами растворителя, в том числе уравнением Кирквуда–Бауэра–Магата (KBM), количеством акцепторов (ANs), уравнением Свейна, линейными соотношениями энергии сольватации (LSER) и квадратным уравнением. Индуцированные растворителем сдвиги $\nu(\text{C=O})$ KETO показывают лучшую корреляцию с LSER, чем с KBM, ANs и уравнением Свейна. Обнаружено, что линейное влияние кислотности донора водородной связи растворителя (A_j) на $\nu(\text{C=O})$ KETO значительно, в то время как основность акцептора водородной связи (B_j) и эффект взаимодействия A_j и B_j несут существенны. Отмечено также, что квадратичные эффекты A_j и B_j незначительны, а линейное влияние параметров LSER (π^ , δ , α и β) и эффект взаимодействия $\pi^*\beta$ на $\nu(\text{C=O})$ KETO существенны.*

Ключевые слова: кетопрофен, эффект растворителя, уравнение Свейна, линейная зависимость энергии сольватации, квадратичное уравнение.

¹ Full text is published in JAS V. 88, No. 4 (<http://springer.com/journal/10812>) and in electronic version of ZhPS V. 88, No. 4 (http://www.elibrary.ru/title_about.asp?id=7318; sales@elibrary.ru).

Introduction. Ketoprofen (KETO), [2-(3-benzoylphenyl)propionic acid], is a benzophenone-derived drug, specifically a nonsteroidal anti-inflammatory drug with antipyretic and analgesic effects [1–3]. For many years, researchers have investigated the vibrational properties of crystalline KETO via experimental techniques, such as inelastic neutron scattering, Raman scattering, and IR spectroscopy [2, 4–6], as well as density functional theory (DFT) calculations [2, 3]. Recently, we investigated whether any clear links exist between the results of the experimental corrosion inhibition [7] efficiencies and the quantum chemical calculations of KETO. However, to the best of our knowledge, theoretical and/or experimental vibrational studies on KETO in solution have not been published so far.

Solvent effects have importance in pharmaceutical manufacturing due to the degrees of absorption, transport, and release of drugs in the human body [8]. The physical and chemical properties of the drug molecules are strongly dependent on the solvent used in the solution [9]. The solvent effects play an important role in many structural parameters such as the vibrational frequencies of the molecules and their intensities [8]. Infrared spectroscopy is an effective method for investigating solvent-induced vibrational frequency shifts [10]. Empirical solvent parameter equations are mainly used to predict shifts in C=O stretching vibrational bands for several organic molecules [10, 11]. The Kirkwood, Bauer, and Magat (KBM) equation, the solvent acceptor numbers (ANs) equation, the Swain equation, and linear solvation energy relationships (LSERs) are used to describe the solvent effects [10–13]. The last two equations are multi-parameter equations.

The KBM model equation is represented [12] as

$$\frac{(\nu^0 - \nu^s)}{\nu^0} = \frac{\Delta\nu}{\nu^0} = \frac{C(\epsilon - 1)}{2\epsilon + 1}, \quad (1)$$

where ϵ is the dielectric constant of a solvent, ν^s and ν^0 are the vibrational frequency of a solute in the solvent and a solute in the gas phase, respectively, and C is a constant depending upon the electrical properties and dimensions of the vibrating solute dipole.

The solvent acceptor numbers (ANs) equation is given [14] as

$$\nu = \nu_0 + K(AN), \quad (2)$$

where ν_0 is the vibrational frequency of the solute in cyclohexane and K is the sensitivity of the vibrational frequency (ν) to solvent AN .

The Swain equation is shown [11, 14] as

$$\nu = \nu_0 + aA_j + bB_j, \quad (3)$$

where ν and ν_0 are the vibration frequency of the solute in the solvent and the predicated vibration frequency in cyclohexane as a reference solvent, respectively, and A_j and B_j are measures of the solvent hydrogen-bond donor acidity and hydrogen-bond acceptor basicity, respectively. The coefficients of a and b symbolize the sensitivity of the solute for the solvent.

The model equation of LSER is represented [11–13] as

$$\nu = \nu_0 + (s\pi^* + d\delta) + a\alpha + b\beta, \quad (4)$$

where ν and ν_0 are the $\nu(\text{C=O})$ of solute in pure solvent and the regression value of the $\nu(\text{C=O})$ in cyclohexane as a reference solvent, respectively; α and β are a measure of the solvent hydrogen bond donor acidity and hydrogen-bond acceptor basicity, respectively; π^* is the index of solvent dipolarity/polarizability; δ is a discontinuous polarizability correction term for polychlorine substituted aliphatic and aromatic solvents; s , d , a , and b are the regression coefficients and provide the susceptibilities of the $\nu(\text{C=O})$ of the solute to the indicated solvent parameters.

The C=O stretching vibrational frequencies of KETO were correlated with the KBM, AN, Swain, and LSER solvent scales. The experimental $\nu(\text{C=O})$ of KETO in several solvents (chloroform, cyclohexane, toluene, benzene, dimethyl sulfoxide, chlorobenzene, dichloromethane, ethanol, methanol, *n*-propanol, *n*-butanol, *i*-propanol, and tert-butanol) were compared with the theoretical $\nu(\text{C=O})$ calculated using empirical solvent parameters. Additionally, the quadratic and interactive effects of solvent parameters on the experimental vibrational spectra of KETO were investigated in this study.

Experimental and computational procedures. KETO (MW, 244.3 g/mol) was purchased from Sigma-Aldrich, USA. All solvents, which were obtained from the Merck, were of analytical or spectroscopic purity and distilled prior to use. For the Fourier transform-infrared (FT-IR) solution spectra, the concentrations of the KETO solution were between 0.075 and 0.080 mol/L. The FT-IR spectra (4000–600 cm^{-1}) of the solutions were recorded using a Bruker Tensor 27 spectrophotometer with a resolution of 2 cm^{-1} and 16 scans.

The FT-IR solution spectra were collected using a diamond attenuated total reflection (ATR) at room temperature (20–23°C). The FT-IR spectra of pure solvents and solid KETO were recorded under the same conditions as the background spectra and were stored on the computer. Opus 6.5 software version was used for all data manipulation.

Results and discussion. *Solvent effects on the experimental vibrational spectra of KETO.* Briard [15] determined the experimental crystal structure of KETO in monomer form in 1990. Its crystal structure can be found (reference code: KEMRUP) [16] in the Cambridge Crystallographic Data Centre (CCDC). The experimental crystal structure and the crystal structure of KETO at the CCDC are shown in Fig. 1.

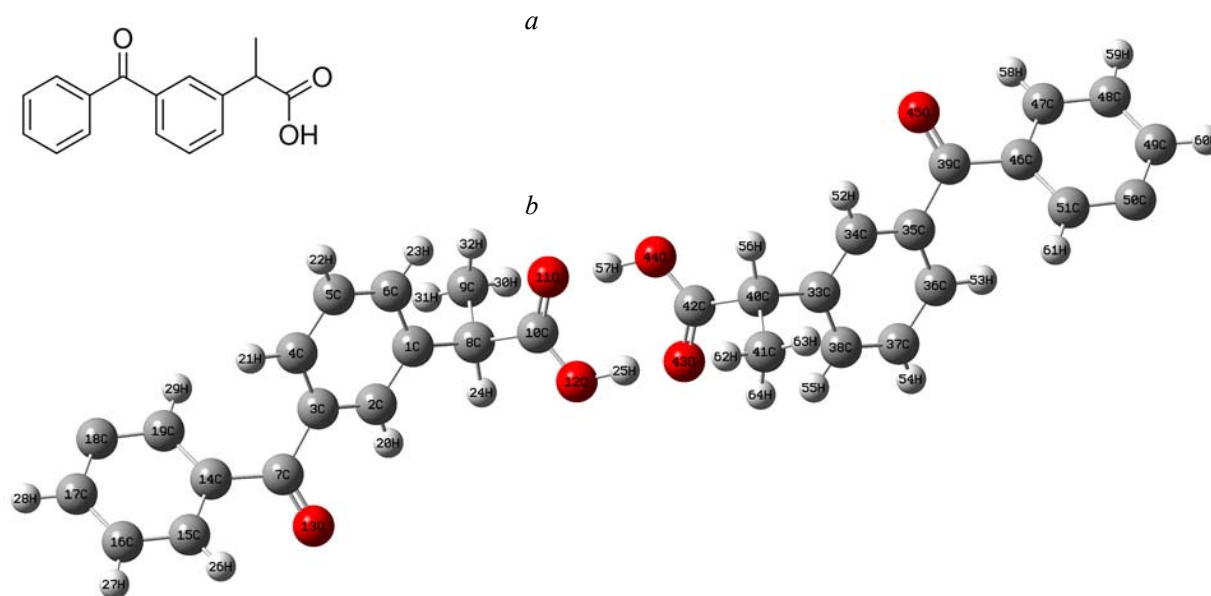


Fig. 1 (a) The experimental crystal structure [15]; (b) the crystal structure [code name: KEMRUP] [16] of KETO at the CCDC.

TABLE 1. The $\nu(\text{C}=\text{O})$ of KETO in Different Solvents and Solvent Parameters

No.	Solvent	$\nu(\text{C}=\text{O})^a$	ϵ	$f(\epsilon)^b$	AN^c	β^d	α^d	π^{*d}	δ^d	A_j^e	B_j^e	$E_T(30)^f$
1	Dimethyl sulfoxide	1716.3	46.45	0.484	19.3	0.76	0	1.0	0	0.34	1.08	45.1
2	Ethanol	1714.9	24.55	0.470	37.9	0.77	0.83	0.54	0	0.66	0.45	51.9
3	Methanol	1715.3	32.66	0.477	41.3	0.62	0.93	0.6	0	0.75	0.50	55.4
4	<i>i</i> -Propanol	1714.4	19.92	0.463	33.6	0.95	0.76	0.48	0	0.59	0.44	48.4
5	<i>n</i> -Propanol	1714.2	20.45	0.464	37.8	0.95	0.76	0.48	0	0.63	0.44	50.7
6	<i>tert</i> -Butanol	1713.6	12.5	0.442	27.1	1.01	0.68	0.41	0	0.45	0.50	43.3
7	<i>n</i> -Butanol	1713.6	17.51	0.458	36.8	0.88	0.79	0.47	0	0.61	0.43	49.7
8	Dichloromethane	1712.6	8.9	0.420	20.4	0	0.185	0.82	0.5	0.33	0.80	40.7
9	Chloroform	1711.9	4.89	0.361	23.1	0.87	0.44	0.58	0.5	0.42	0.73	39.1
10	Chlorobenzene	1707.2	5.74	0.379	8.0	0.07	0	0.65	1.0	0.20	0.65	36.8
11	Toluene	1706.5	2.38	0.239	8.6	0.11	0	0.54	0.7	0.13	0.54	33.9
12	Benzene	1706.7	2.27	0.229	8.2	0.1	0	0.59	0.8	0.15	0.59	34.3
13	Cyclohexane	1700.2	2.02	0.202	0	0	0	0	0	0.02	0.06	30.9

^a The experimental $\nu(\text{C}=\text{O})$ stretching frequencies (cm^{-1}) of KETO.

^b $f(\epsilon) = (\epsilon - 1)/(2\epsilon + 1)$.

^c Solvent acceptor number.

^d Parameters of LSER solvent equation.

^e Parameters of Swain solvent equation.

^f Empirical parameters of solvent polarity, $E_T(30)$ (kcal/mol).

Figure 2 displays the experimental IR spectra of KETO in 13 pure solvents. The strong peak in the IR spectra was found to come from the $\nu(\text{C}=\text{O})$ mode. The $\nu(\text{C}=\text{O})$ stretching bands of KETO in the solvents appear in the region of $1700\text{--}1717\text{ cm}^{-1}$. Figure 2 also shows the frequency shifts and changes in the IR intensity of $\nu(\text{C}=\text{O})$ from the solid state (the experimental value is 1695 cm^{-1} for the solid state) to the various solvents. The observed carbonyl stretching vibrational frequencies of KETO in 13 pure solvents along with the solvent parameters are presented in Table 1. In Table 1, $E_T(30)$ is the solvent polarity parameter proposed by Dimroth and Reichardt. Generally higher $E_T(30)$ values correspond to a higher solvent polarity [13]. For KETO/cyclohexane, the carbonyl vibration is computed at lower frequency, whereas frequency bands have been observed at higher frequencies in polar solvents.

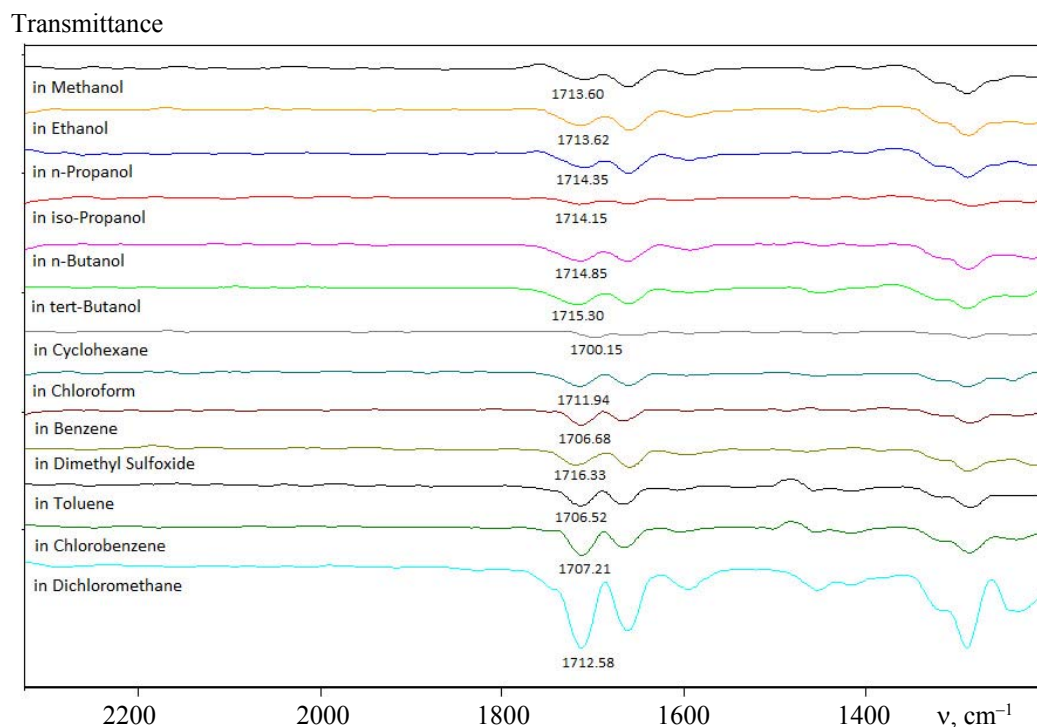


Fig. 2. The experimental FT-IR spectra of KETO in 13 pure solvents.

It is found from the plot (Fig. 3a) of the experimental $\nu(\text{C}=\text{O})$ of KETO versus $(\epsilon-1)/(2\epsilon+1)$ of the KBM equation that a good relationship exists between the experimental $\text{C}=\text{O}$ stretching vibrational frequencies of KETO and the KBM parameters (Table 1), as the frequency shifts depend on the solvent dielectric constant. The plot (Fig. 3b) of $\nu(\text{C}=\text{O})$ of KETO versus the solvent ANs shows a good correlation due to the role of solvents (Table 2). It was also found that when increasing solvent ANs, $\nu(\text{C}=\text{O})$ of KETO shifts to lower frequencies, and this trend verifies the presence of some specific interaction between KETO and polar solvents [17].

The Swain equation for the $\nu(\text{C}=\text{O})$ of KETO is given in Table 2. Swain equations include the hydrogen-bond donor acidity and hydrogen-bond acceptor basicity of the solvent and are used for describing specific solvent effects, such as electron pair transfer and H-bond [18]. The correlation of the Swain equation for the $\nu(\text{C}=\text{O})$ of KETO is very good and better than that of the ANs of the solvents due to considering the Lewis acidity and basicity for the solvent. The positive signs for A_j and B_j indicate that the increase in hydrogenbond donor acidity and hydrogen-bond acceptor basicity of the solvent leads to the blue shift of the $\nu(\text{C}=\text{O})$ of KETO. The blue shift of the $\nu(\text{C}=\text{O})$ of the KETO band induced by hydrogen-bond donor acidity is larger than that induced by the hydrogen-bond acceptor basicity of the solvent, as the ratios of A_j and B_j are almost equal to 2.

The LSER parameters are also given in Table 2. The results of LSERs that have excellent correlations exhibit better correlations than the results found through the KBM equation, the ANs of the solvents, and the Swain equation. The LSER model takes into account not only the specific interaction parameters (α and β) but also the nonspecific interaction parameter (π^*) [10]. The positive π^* coefficients show a blue shift of the

$\nu(\text{C=O})$, when one observes nonspecific solvent effects. The π^* coefficients with the biggest absolute values prove that nonspecific solvent effects are dominant in the compound/solvent interactions. The coefficients of α and β are also positive, and a similar result was found for the A_j and B_j parameters in the Swain equation. This indicates the same influence by the hydrogen-bond donor acidity and hydrogen-bond acceptor basicity of the solvent with regard to the blue-shift of the carbonyl vibrations. Note that the α coefficients are larger than the β coefficients. The carbonyl vibration of KETO is more susceptible to the hydrogen-bond donor acidity and hydrogen-bond acceptor basicity of the solvent.

TABLE 2. Solvent Equations for the $\nu(\text{C=O})$ of KETO

KBM $(1694.55 \pm 2.03) + (42.90 \pm 5.04)f(\epsilon)$	$R^2 = 0.8683$
AN $(1704.50 \pm 1.41) + (0.29 \pm 0.05)\text{AN}$	$R^2 = 0.7402$
Swain $(1699.05 \pm 1.01) + (17.33 \pm 1.40)A_j + (9.46 \pm 1.38)B_j$	$R^2 = 0.9521$
LSER $(1700.33 \pm 0.50) + [(14.23 \pm 0.73)\pi^* - (2.54 \pm 0.59)\delta] + (5.84 \pm 0.65)\alpha + (2.64 \pm 0.65)\beta$	$R^2 = 0.9921$

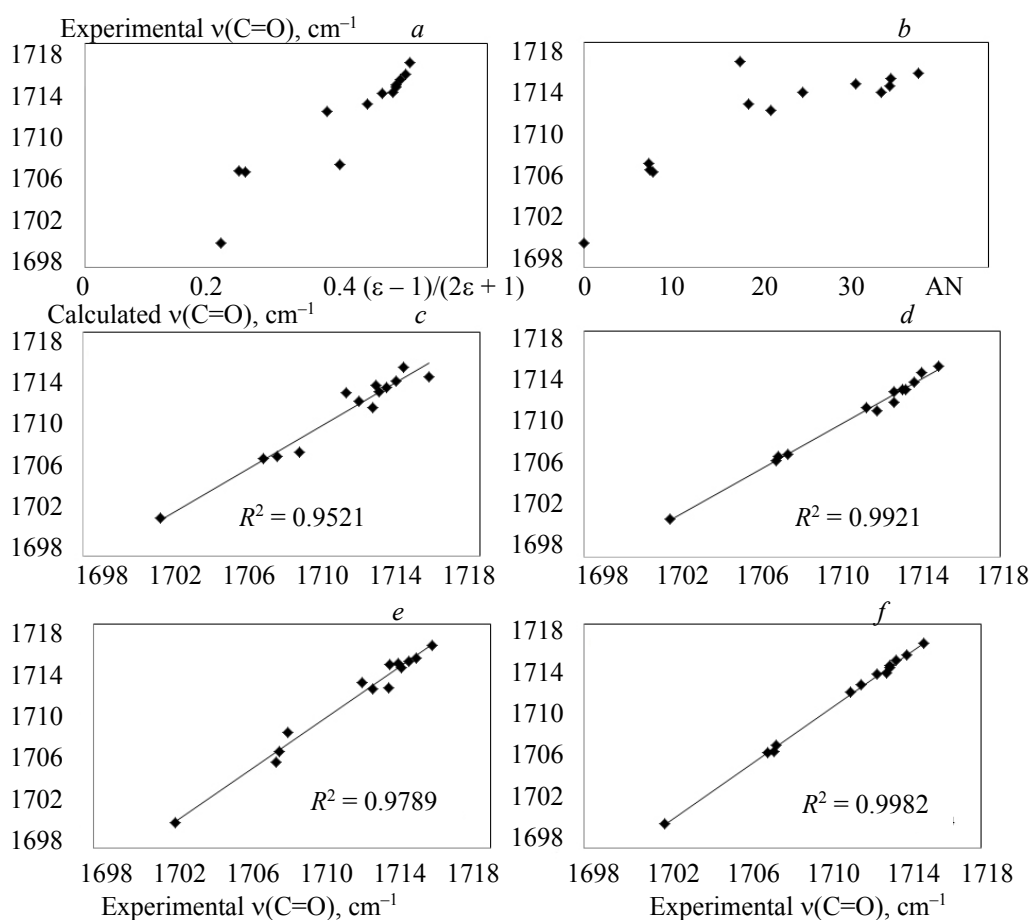


Fig. 3. Plot of (a) KBM and (b) AN parameters vs. the experimental C=O stretching vibrational frequencies of KETO, and validation regression plots of the $\nu(\text{C=O})$ of KETO calculated using (c) the linear Swain equation, (d) the linear LSER equation, (e) the quadratic Swain equation, and (f) the quadratic LSER equation vs. experimental values.

The $\nu(\text{C=O})$ of KETO achieves excellent correlations with the parameters of the LSER equation. It is suggested that nonspecific solvent effects between KETO and solvents play a dominant role due to the large coefficient of the π^* value. Compared with the KBM equation, the ANs of the solvents, and the Swain equation, the LSER equation offers a quantitatively accurate and physically meaningful explanation of solvent-

induced stretching frequency shifts. The success of the model equations of the Swain equation and the LSER equation applied to FT-IR spectroscopy are illustrated in Figs. 3c,d. As a result, the LSER is suitable for investigating the solute and solvent interactions in all solvents.

Interactive and quadratic effects of solvent parameters on the experimental vibrational spectra of KETO. The Swain and LSER equations are multi-parameter treatments used to describe the solvent effects on the vibrational spectra of organic molecules. The Swain and LSER equations include the main effects of solvent parameters on the vibrational spectra. In this study, the linear, quadratic, and interactive effects of solvent parameters on the experimental vibrational spectra of KETO were investigated, unlike in similar studies in the literature. The interactive effects of solvent parameters were determined using multi-parameter regression via MINITAB 18 (USA).

The solvent effects on the $\nu(\text{C}=\text{O})$ of KETO for the Swain equation are explained by the following quadratic:

$$\nu = \nu_0 + \beta_1 A_j + \beta_2 B_j + \beta_{11} A_j^2 + \beta_{22} B_j^2 + \beta_{12} A_j B_j, \quad (5)$$

where the predicted frequency (ν) was therefore correlated to the set of regression coefficients: the intercept (ν_0), linear (β_1, β_2), quadratic (β_{11}, β_{22}), and interaction (β_{12}) coefficients. Coefficients of the respective effects were represented by β and were determined by applying the Student's t -test. The MINITAB 18 was used for the regression and graphical analysis of the data. The regression coefficient, the standard deviation of each coefficient, and the t and P values for all of the linear, quadratic, and interaction effects of the parameter determined from the analysis of the data are displayed in Table 3 for the Swain equation.

The coefficient of determination (R^2) ensured a satisfactory adjustment of the quadratic model to the experimental $\nu(\text{C}=\text{O})$ of KETO in the present study. The use of the coefficient of determination ($R^2 = 0.9789$) and the adjusted determination coefficient (adjusted $R^2 = 0.9639$) for the quadratic model, the most appropriate model, showed a better correlation (Fig. 3e) when compared with the linear model ($R^2 = 0.9521$) given in Table 2.

The regression equation for the $\nu(\text{C}=\text{O})$ of KETO is given as

$$\nu = 1699.59 + 43.39 A_j - 2.36 B_j - 20.39 A_j^2 + 12.02 B_j^2 - 20.00 A_j B_j. \quad (6)$$

A larger magnitude of t and a smaller value of P indicates that the model is considered to be statistically significant (with a 95% confidence level) [19]. The linear effect of A_j ($P = 0.003$) on the $\nu(\text{C}=\text{O})$ of KETO was found to be highly significant, whereas B_j ($P = 0.623$) was not significant. Additionally, it was observed that the quadratic effects of A_j (0.053) and B_j (0.063) were slightly significant, but the interaction effect of A_j and B_j ($P = 0.221$) was not considered to be a significant factor. The significant interactive effects of A_j and B_j for the Swain equation are represented in the form of three-dimensional (3D) surface plots and contour plots in Fig. 4a,b. The linear effect of A_j on the $\nu(\text{C}=\text{O})$ of KETO was the most significant effect, and the result closely agreed with that obtained from the Swain equation. Therefore, the model including the linear, quadratic, and interaction effects of the parameters can be effectively used to investigate the solvent effects on the $\nu(\text{C}=\text{O})$ of KETO.

TABLE 3. Regression Model Results for the Swain and the LSER Equations

Term	Coefficient	Standard Error	t	P
Swain Equation				
Constant	1699.59	1.07	1593.23	0.000
A_j	43.39	9.86	4.40	0.003
B_j	-2.36	4.58	-0.51	0.623
A_j^2	-20.39	8.76	-2.33	0.053
B_j^2	12.02	5.46	2.20	0.063
$A_j B_j$	-20.0	14.9	-1.34	0.221
LSER Equation				
Constant	1700.13	0.25	6758.99	0.000
π^*	16.53	0.59	28.19	0.000
δ	-3.96	0.41	-9.67	0.000
α	4.12	0.47	8.74	0.000
β	6.62	0.86	7.69	0.000
$\pi^* \beta$	-7.05	1.41	-4.99	0.002

The solvent effects on the $\nu(\text{C}=\text{O})$ of KETO for the LSER equation are explained by the following quadratic:

$$\vartheta = \vartheta_0 + k_1\pi^* + k_2\delta + k_3\alpha + k_4\beta + k_{11}\pi^{*2} + k_{22}\delta^2 + k_{33}\alpha^2 + k_{44}\beta^2 + k_{12}\pi^*\delta + k_{13}\pi^*\alpha + k_{14}\pi^*\beta + k_{23}\delta\alpha + k_{24}\delta\beta + k_{34}\alpha\beta, \quad (7)$$

where the predicted frequency (ν) is correlated to the set of regression coefficients: the intercept (ϑ_0), linear (k_1, k_2, k_3, k_4), quadratic ($k_{11}, k_{22}, k_{33}, k_{44}$), and interaction ($k_{12}, k_{13}, k_{14}, k_{23}, k_{24}, k_{34}$) coefficients. The coefficients of the respective effects are represented by k and were determined by applying the Student's t -test. The MINITAB 18 was used for regression and the graphical analysis of the data. The regression coefficient, standard deviation of each coefficient, and t and P values for the parameters determined from the analysis of the data are displayed in Table 3 for the LSER equation.

The use of the coefficient of determination ($R^2 = 0.9982$) and the adjusted determination coefficient (adjusted $R^2 = 0.9970$) for the quadratic model showed a better correlation (Fig. 3f) when compared with the linear model ($R^2 = 0.9921$) given in Table 2.

The experimental data demonstrated that the other quadratic and interaction terms, except for the term of $\pi^*\beta$, were not significant ($P > 0.05$). Thus, the reduced regression equation for the $\nu(\text{C}=\text{O})$ of KETO is

$$\vartheta = 1700.13 + 16.53\pi^* - 3.96\delta + 4.12\alpha + 6.62\beta - 7.05\pi^*\beta. \quad (8)$$

The linear effect of π^* ($P < 0.001$), δ ($P < 0.001$), α ($P < 0.001$), and β ($P < 0.001$), as well as the interaction effect of $\pi^*\beta$ ($P = 0.002$) on the $\nu(\text{C}=\text{O})$ of KETO, were found to be highly significant. The significant interactive effects of $\pi^*\beta$ for the LSER equation are represented in the form of 3D surface plots and contour plots in Fig. 4c,d. The linear effect of π^* on the $\nu(\text{C}=\text{O})$ of KETO was the most significant effect, and the result closely agree with that obtained from the LSER equation. Therefore, the model including the linear and interaction effects of the parameters can be effectively used to investigate the solvent effects on the $\nu(\text{C}=\text{O})$ of KETO.

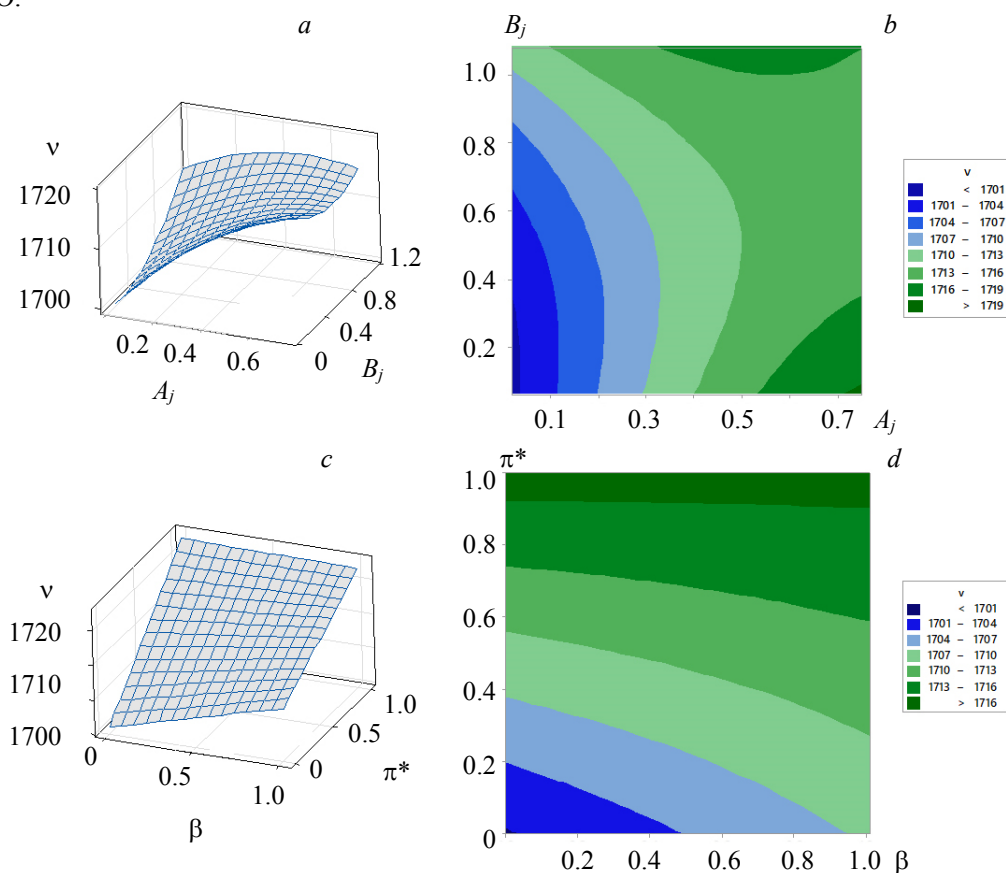


Fig. 4. (a) 3D surface plot and (b) contour plot for the combined effect of A_j and B_j parameters; (c) 3D surface plot and (d) contour plot for the combined effect of π^* and β parameters on the $\nu(\text{C}=\text{O})$ frequencies of KETO.

Conclusions. The solvent effects on the $\nu(\text{C}=\text{O})$ of KETO in 13 solvents are investigated through FT-IR experiments. FT-IR spectroscopy is utilized to record the solvent-induced $\nu(\text{C}=\text{O})$ of KETO. The results of this study are as follows: (i) the experimental IR spectra of KETO in the solvents show the frequency shifts and change in the IR intensity of $\nu(\text{C}=\text{O})$ from the solid state to the various solvents; (ii) for the solvent-induced $\nu(\text{C}=\text{O})$ of KETO, the KBM ($R^2 = 0.8683$) and the solvent ANs ($R^2 = 0.7402$) of the solvents were found to have good correlations with the theoretical values; (iii) the $\nu(\text{C}=\text{O})$ of KETO achieved a very good linear correlation with the Swain equation ($R^2 = 0.9521$), whereas the LSER equation ($R^2 = 0.9921$) showed excellent correlation analysis results for the $\nu(\text{C}=\text{O})$ of KETO in all solvents; and (iv) the LSER equation offers a quantitatively accurate and physically meaningful explanation of solvent-induced stretching frequency shifts. This fact allows for the prediction of the $\nu(\text{C}=\text{O})$ of KETO in other solvents if the LSER parameters of these solvents are obtained; (v) quadratic equations were applied for the Swain ($R^2 = 0.9789$) and LSER ($R^2 = 0.9982$) equations in order to predicting the $\nu(\text{C}=\text{O})$ of KETO in pure solvents. The quadratic equation provided more accurate predictions than the linear Swain and LSER equations.

Acknowledgement. The authors would like to thank the Kocaeli University Research Fund for financial support (Grant No. 2012/069).

REFERENCES

1. J. Y. Song, S. H. Jhung, *Chem. Eng. J.*, **322**, 366–374 (2017).
2. M. L. Vueba, M. E. Pina, F. Veiga, J. J. Sousa, L. A. E. Batista de Carvalho, *Int. J. Pharm.*, **307**, 56–65 (2006).
3. T. Shibata, H. Igawa, T. H. Kim, T. Mori, S. Kojima, *J. Mol. Struct.*, **1062**, 185–188 (2014).
4. S. H. Choi, S. Y. Kim, J. J. Ryoo, J. Y. Park, K. P. Lee, *Anal. Sci.*, **17**, 785–788 (2001).
5. L. A. E. Batista de Carvalho, M. Paula, M. Marques, J. Tomkinson, *Biopolymer*, **82**, 420–424 (2006).
6. Y. H. Lu, C. B. Ching, *Chirality*, **16**, 541–548 (2004).
7. F. Kayadibi, S. Zor, S. G. Sagdinc, *Prot. Met. Phys. Chem. S.*, **52**, 355–370 (2016).
8. M. T. Bilkani, O. Şahin, Ş. Yurdakul, *J. Mol. Struct.*, **1133**, 580–590 (2017).
9. T. Polat, G. Yıldırım, *Spectrochim. Acta A-M.*, **123**, 98–109 (2014).
10. N. Tekin, H. Pir, S. Sagdinc, *Spectrochim. Acta A-M.*, **98**, 122–131 (2012).
11. Y. Chen, H. Zhang, Q. Liu, *Spectrochim. Acta A-M.*, **126**, 122–128 (2014).
12. X. Ji, Y. Li, J. Zheng, Q. Liu, *Mater. Chem. Phys.*, **130**, 1151–1155 (2011).
13. C. Reichardt, *Solvents and Solvent Effects in Organic Chemistry*, Wiley-VCH Verlag GmbH & Co. KGaA, Weinheim, 418–424 (2003).
14. M. Tursun, C. Parlak, *Spectrochim. Acta A-M.*, **141**, 58–63 (2015).
15. P. Briard, J. Rossi, *Acta Crystallogr. C*, **46**, 1036–1038 (1990).
16. *Cambridge Crystallographic DataBase*, Cambridge Crystallographic Data Center, Cambridge UK.
17. C. Conti, R. Galeazzi, E. Giorgini, G. Tosi, *J. Mol. Struct.*, **744–747**, 417–423 (2005).
18. Q. Liu, C. Cong, H. Zhang, *Spectrochim. Acta A*, **68**, 1269–1273 (2007).
19. S. M. Rafigha, A. V. Yazdia, M. Vossoughib, A. A. Safekordia, M. Ardjmand, *Int. J. Biol. Macromol.*, **70**, 463–473 (2014).